Mediterranean Thematic Workshops in Advanced Molecular Imaging

MEDAMI 2016 - IV Mediterranean Thematic Workshop in Advanced Molecular Imaging

Ajaccio , 1-5 May 2016

Past, Present and Future of PET

Alberto Del Guerra

Functional Imaging and Instrumentation Group
Dipartimento di Fisica "E. Fermi"
Universita' di Pisa and INFN, Sezione di Pisa

http://www.df.unipi.it/~fiig/
Email:alberto.del.guerra@unipi.it

FIIG

IN SUPREMÆ DIGNITATIS 1343

Content

- The Evolution of PET
- Clinical applications (PET-CT)
- Preclinical Systems
  - (From man to mice ….and back)
- Hybrid Systems (PET-MR)
- PET range monitoring in particle therapy
- The future of PET➔take home messages
- Conclusions

The EVOLUTION of PET

The first idea of PET
(talk at MGH by William Sweet, May 16,1951)

First Clinical Positron Imaging Device

1953 - This instrument followed the general concepts of the instrument build in 1950 but included many refinements. It produced both a coincidence scan as well as an unbalance scan. The unbalance of the two detectors was used to create an unbalance image using two symbols to record any unbalance in the single channel rates of the two detectors.

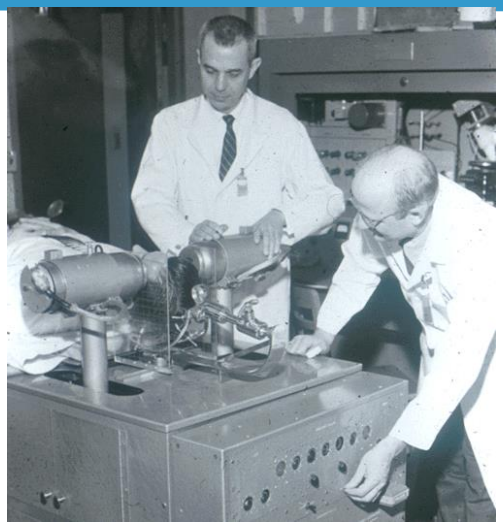

Dr. Brownell (left) and Dr.Aronow are shown with the scanner (1953).

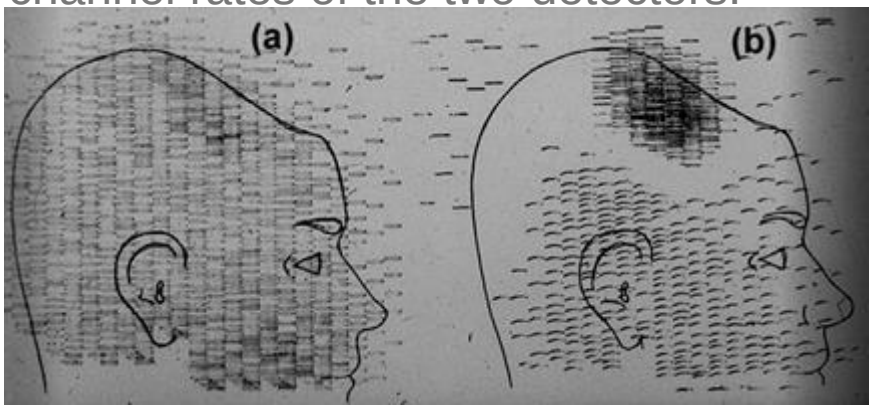

Coincidence and unbalance scans of patient with recurring brain tumor. Coincidence scan (a) of a patient showing recurrence of tumor under previous operation site, and unbalance scan (b) showing asymmetry to the left. (Reproduced from Brownell and Sweet 1953).

A.Del Guerra et al., Rivista Nuovo Cimento [2016, Vol. 39(4), pp.155-223]

The main performance parameters of a PET scanner

- **Sensitivity**
- **Spatial resolution**
- **Time resolution**
- **Reconstruction Algorithm**
- **Correction and Quantitation**
- **Specificity of the radiotracer**

Evolution of the *Scintillators*
(sensitivity and time resolution)

	NaI	BGO	GSO	LSO	LYSO	LGSO	LuAP	YAP	$LaBr_3$
Light yield 10^3 ph/MeV	38	9	8	30	32	16	12	17	60
Primary decay time	250	300	60	40	41	65	18	30	16
ΔE/E (%) at 662 keV	6	10	8	10	10	9	15	4.4	3
Density (g/cm^3)	3.67	7.13	6.71	7.35	7.19	6.5	8.34	5.5	5.08
Effective Z_{eff}	50	73	58	65	64	59	65	33	46
1/μ @ 511 keV (mm)	25.9	11.2	15.0	12.3	12.6	14.3	11.0	21.3	22.3
PE (%) at 511 keV	18	44	26	34	33	28	32	4.4	14

[A.Del Guerra et al., Rivista Nuovo Cimento [2016, Vol. 39(4), pp.155-223]

Evolution of *PET scanner geometry*: From Single Ring to Multiring From 2D to 3D

Single ring
4 cm - 6 cm
axially

Multiring
Around 20 cm
axially

Multiring 2D w/ septum

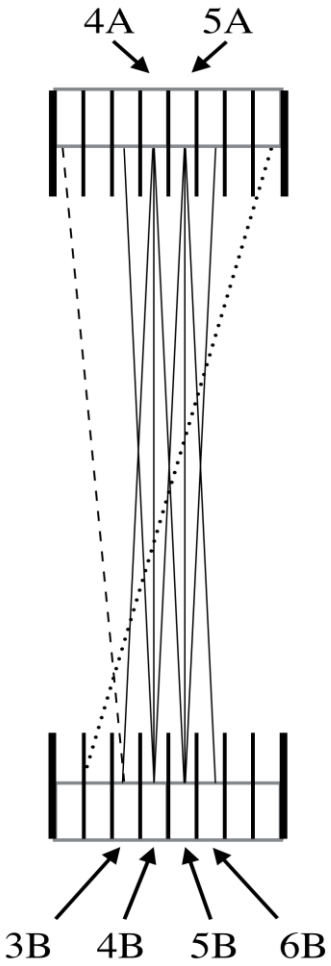

Multiring 3D w/o septum

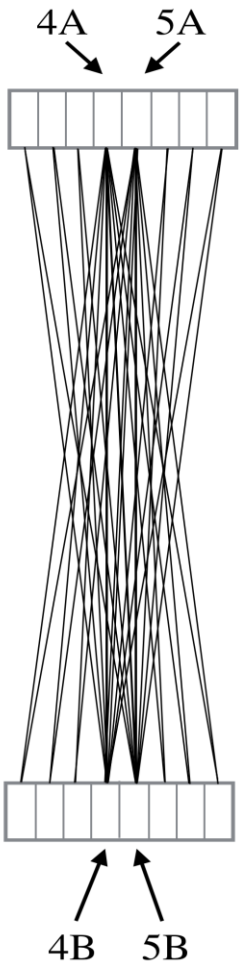

Evolution of the *Photodetectors*
(spatial and time resolution)

- **PhotoMulTiplier (PMT)**
- **Position Sensitive PhotoMulTiplier (PSPMT)**
  - **Round 2” (e.g. R2486)**
    (proximity mesh dynodes and crossed wire anode)
  - **Square 1” (e.g. R7600-C8, R5900-C12)**
    (metal channel dynodes and crossed plate anode)
  - **Square 2” – Flat panel (e.g. H8500)**
    (metal channel dynodes and multi-anode)

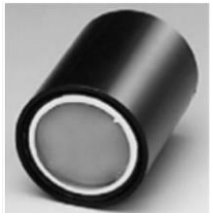

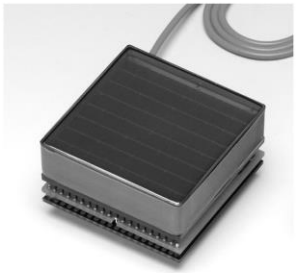

- **Solid State Detectors (SSD)**
  - **Avalanche Photo-Diode (APD and PSAPD)**
  - **Silicon Photo-MultiPlier (SiPM)**
    - **Analog SiPM**
    - **Digital SiPM**

Development of SiPMs geometry (@FBK-irst, Trento, Italy) May 2007

Different geometry,size,microcell size and GF.

$40x40\mu m^2$ => GF 44%
$50x50\mu m^2$ => GF 50%
$100x100\mu m^2$ => GF 76%

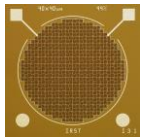

1mm ϕ

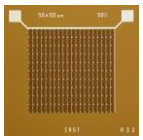
1x1mm²

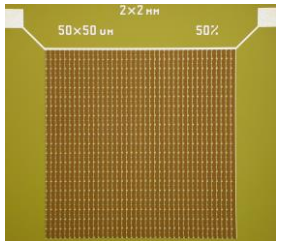

2x2mm²

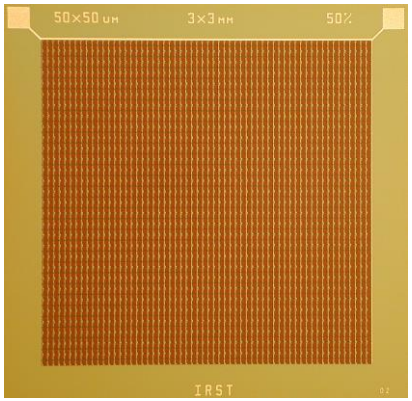

3x3mm² (3600 cells)

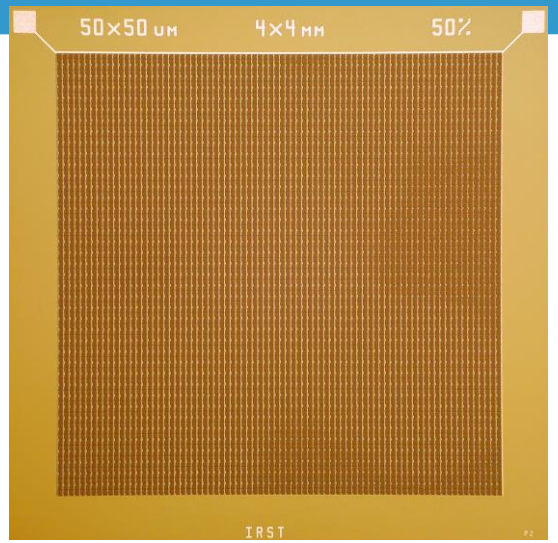

4x4mm² (6400 cells)

Matrices 16 elements (4x4)

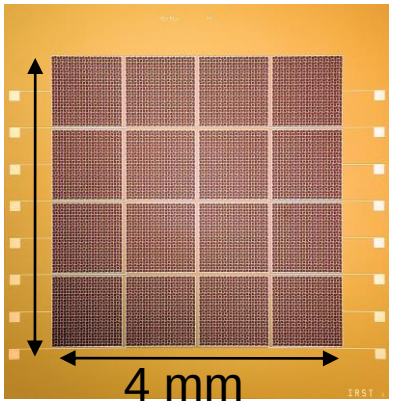

IV CURVES OF 9 MATRICES.

VERY UNIFORM BREAKDOWN POINT

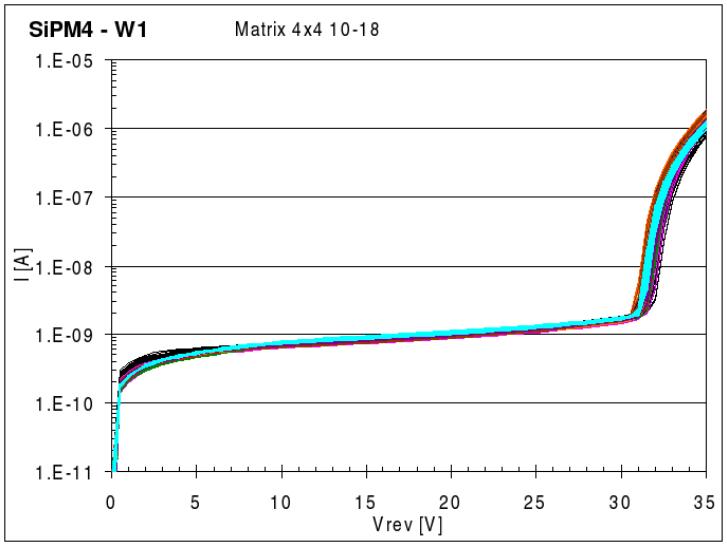

[C.Piemonte et al, Il Nuovo Cimento C, 2007,30(5),473-482]

Spatial Resolution

$$FWHM = 1.25\sqrt{\left(\frac{d}{2}\right)^2 + b^2 + (0.0022D)^2 + r^2 + p^2}$$

1.25	**from analytical algorithm (FBP)**
d/2	**from the detector pitch**
b	**from the coding**
0.0022D	**from the 2 photons a-collinearity**
r	**from the positron range**
p	**from parallax**

Evolution of ***Scintillator to Photodetector coupling*** (spatial resolution)

- **1 Block to 1 PMT (low granularity) [1951]**
- **1 Block w/cuts to some PMTs [1986]**
- **1 Matrix to 1 PSPMT [1990]**
- **1 Pixel to 1 SSD pixel (high granularity)**

  1 Matrix to 1 SSD Matrix [1995➔ to date]
- **1 Monolithic to 1 SSD Matrix (high granularity)**

  [2000➔ to date]

Time Resolution

- Coincidence measurement with two LSO crystals (1x1x10 mm^3) coupled to two SiPMs
- {from: Post and Schiff, Phys. Rev. 80 (1950)1113}

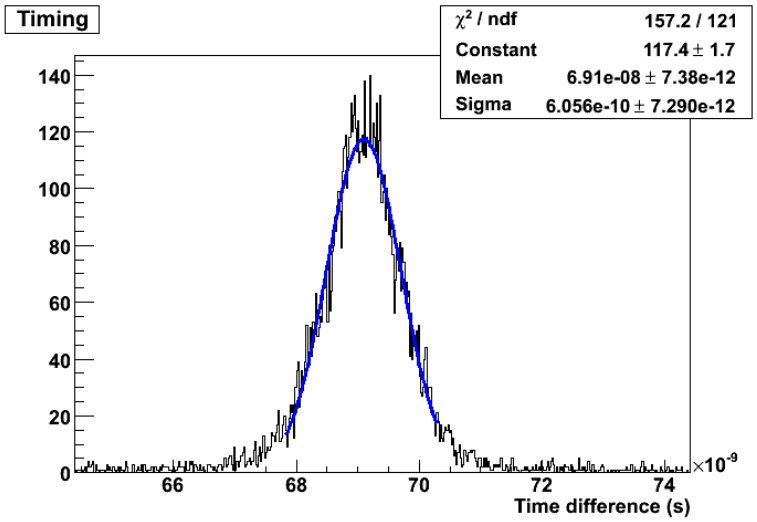

$$\sigma \sim \frac{\sqrt{Q}\,\tau}{< N >}$$

Where:

<N> = average number of photons: ~ 100 photons at the photopeak

Q = Trigger level: ~1 photoelectron.

τ = Decay time of the scintillator (40ns)

For the two scintillators in coincidence calculated : => $\sqrt{2}\sigma$~ 630 ps .

Measured => ~ 600 ps sigma.

[G.Llosa,et al., IEEE Trans. Nucl. Sci. 2008, 55(3), 877-881.

Time of flight PET (TOFPET)

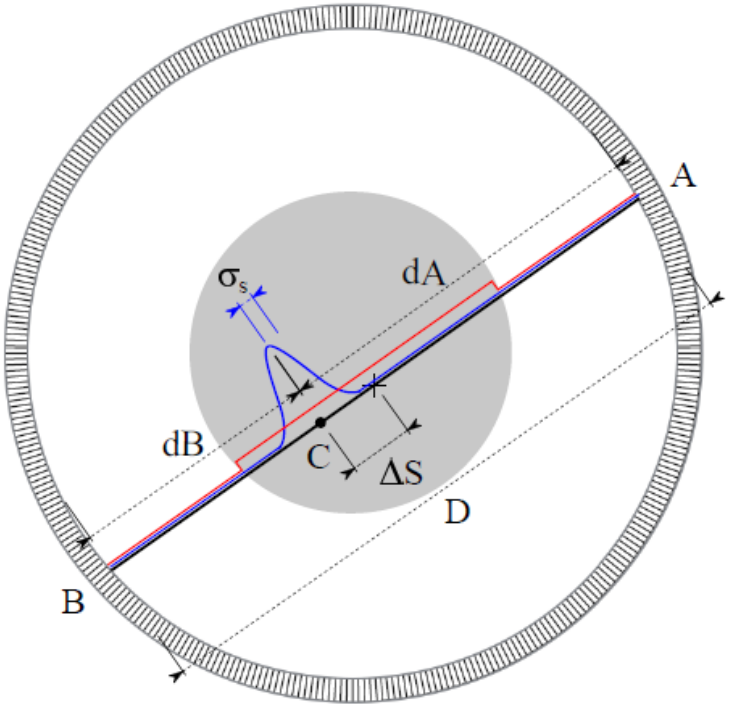

Figure 18.: The Time-of-Flight PET concept. The displacement of the annihilation point along the LOR (ΔS) is obtained by measuring the difference in arrival time ΔT (see text). Blue and red lines show how data are distributed along the LOR during the retroprojection step. Non-TOF data (red) are uniformily distributed along the LOR while TOF-data are distributed around the emission point thus increasing SNR in the reconstructed image.

[A.Del Guerra et al., Rivista Nuovo Cimento [2016, Vol. 39(4), pp.155-223]

The evolution of the *algorithms*

Analytical Methods

- **2-D: Filtered Back-Projection (FBP) [Shepp and Logan, 1974]**
  1. Unidimensional Fourier transform of each projection
  2. Filtering each projection in the unidimensional Fourier space by multiplying by the frequency filter (|ν| ,i.e.,Ram-Lak; Hamming; Shepp-Logan)
  3. Inverse unidimensional Fourier transform of each filtered projection
  4. Projecting backward the filtered projections
- **3-D: Single Slice Re-Binning (SRB);**
  Fourier Rebinning (FORE)
  3-D Filtered Back-Projection (FBP)

Iterative Methods (2D & 3D)

- **Maximum Likelihood Expectation Maximization (ML-EM) [Shepp and Vardi, 1982]**
- **Ordered Subsets Expectation Maximization (OSEM) [Hudson and Larkin, 1994]**

Evolution of the *Correction and Quantitation*

- **Radioisotope Decay Time correction**
- **Dead-time (DAQ,..) correction**
- **Partial volume (PV) correction, i.e., (RC)**
- **Attenuation correction with a 68-Ge rod**
- **Attenuation correction with a low dose, non-diagnostic CT, i.e. ➔PET-CT**
- **Random subtraction**
- **Scatter subtraction**
- **Scatter correction in ML-EM**
- **Complete PSF (system matrix) in ML-EM**

The evolution of the radiotracers (specificity)

TABLE III.: Physical properties of the so-called physiological radioisotopes

Radioisotope	Half-life (min)	Positron average kinetic energy (MeV)	Positron kinetic energy endpoint (MeV)	Positron average range in water (mm)
^{11}C	20.4	0.385	0.960	1.2
^{13}N	10.0	0.491	1.198	1.6
^{15}O	2.0	0.735	1.732	2.8
^{18}F	109.8	0.242	0.633	0.6

RADIOTRACERS

- ^{18}F based — ^{18}F-FDG: metabolism (a-specific)
  ^{18}F-FLT: cell proliferation
  ^{18}F-MISO: hypoxia
  ^{18}F-DOPA: Parkinson... and more
- ^{11}C- based — ^{11}C-choline:prostate
  Pittsburgh compound B (Alzheimer)... and more
- ^{13}N, ^{68}Ga, ^{64}Cu-based .. and more

[A.Del Guerra et al., Rivista Nuovo Cimento [2016, Vol. 39(4), pp.155-223]

Clinical applications

Oncology

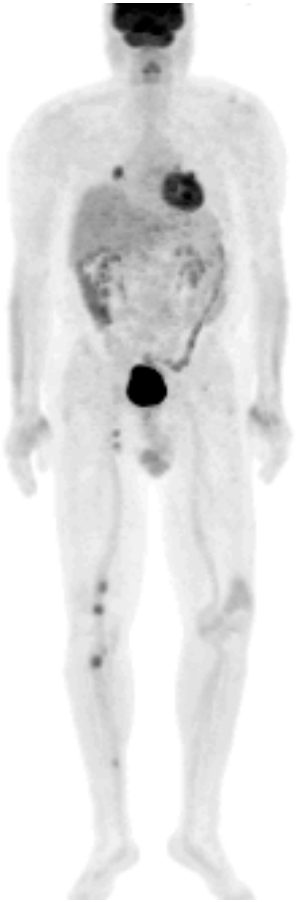

^{18}F-FDG
Total body

Neurology

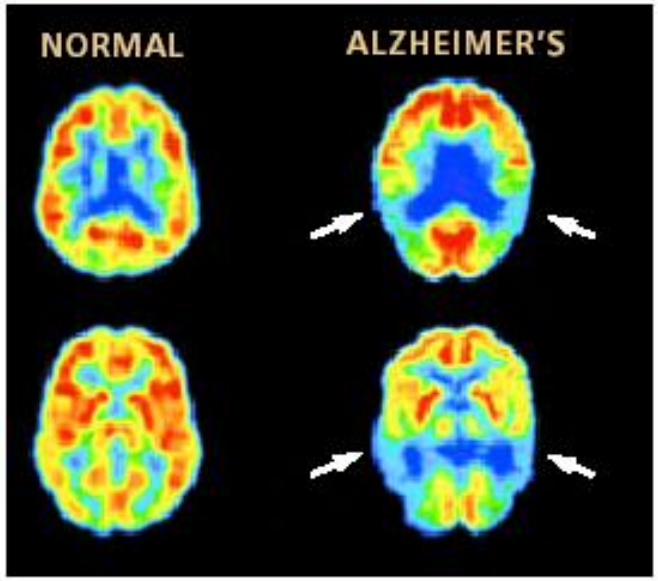

^{18}F-FDG
Brain study for
Alzhemeir's disease

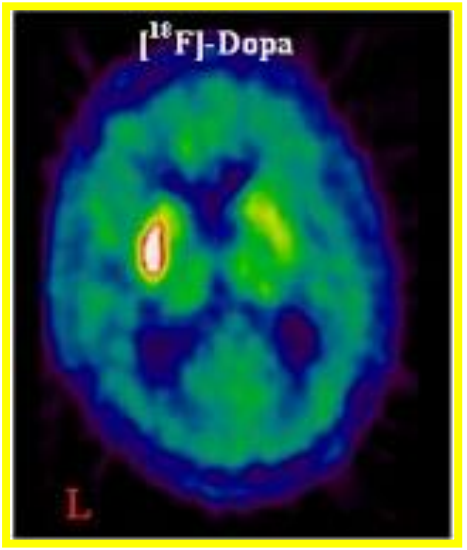

^{18}F-DOPA
Brain study for
Parkinsons's disease

Response to chemotherapy w/FDG

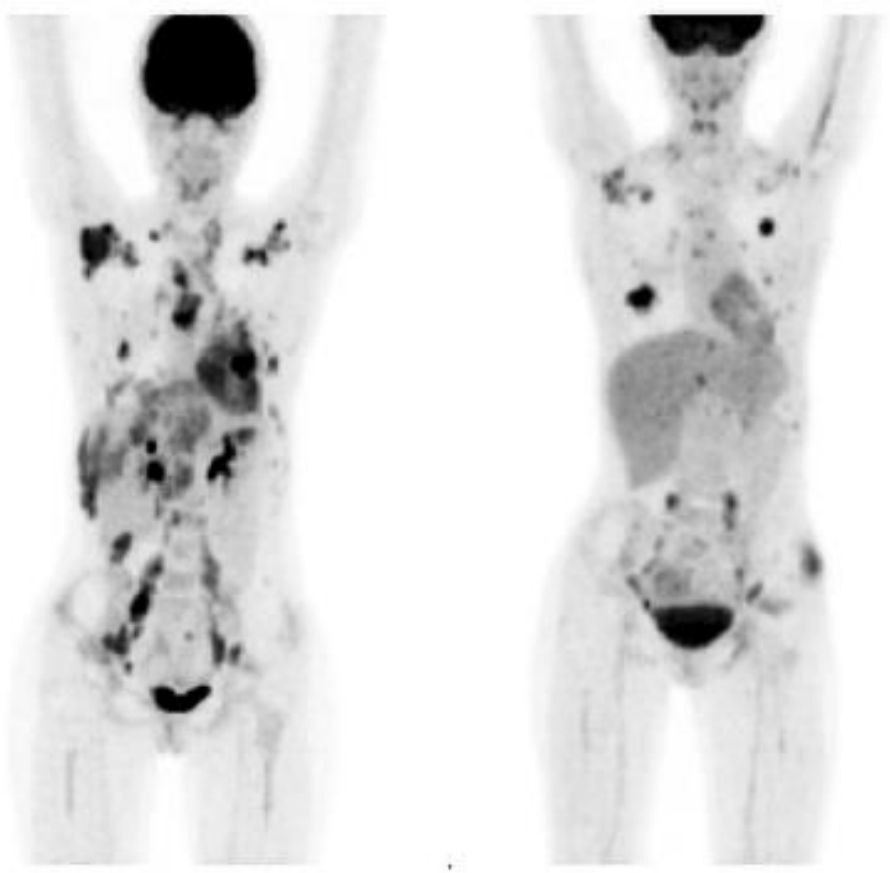

Figure 20.: ^{18}F-FDG PET/CT for the evaluation of the response to chemotherapy in a patient with Hodgkin Lymphoma, see text. (Courtesy of Paola Erba, University of Pisa, 2014). **[A.Del Guerra et al,. Rivista Nuovo Cimento [2016, Vol. 39(4), pp.155-223]**

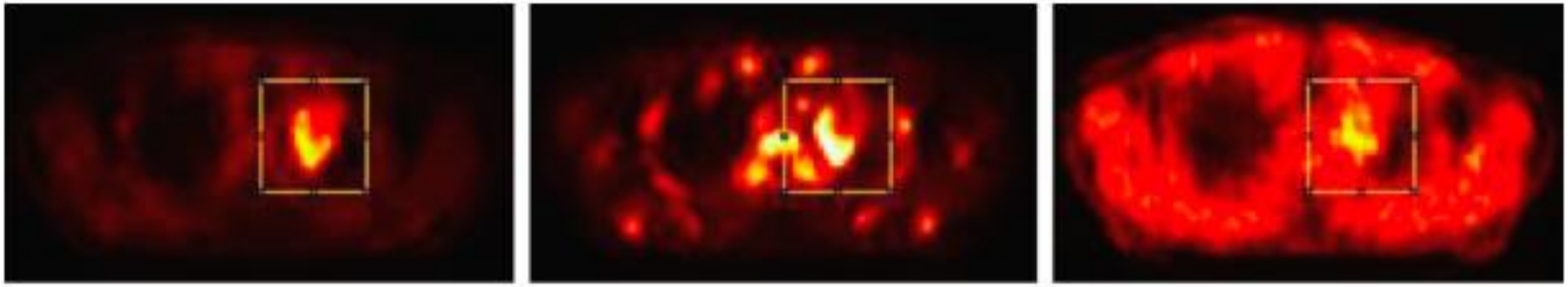

(a) FDG (b) FLT (c) FMiso

Example of varying uptake (indicated by the yellow box) and background activity patterns in PET images of the same patient with a centrally located lung tumor, highlighting the different functional properties of the applied 18F-based tracers [(a) FDG, (b) FLT, and (c) FMISO]
[K.Parodi, Medical Physics, Vol. 42, No. 12, December 2015]

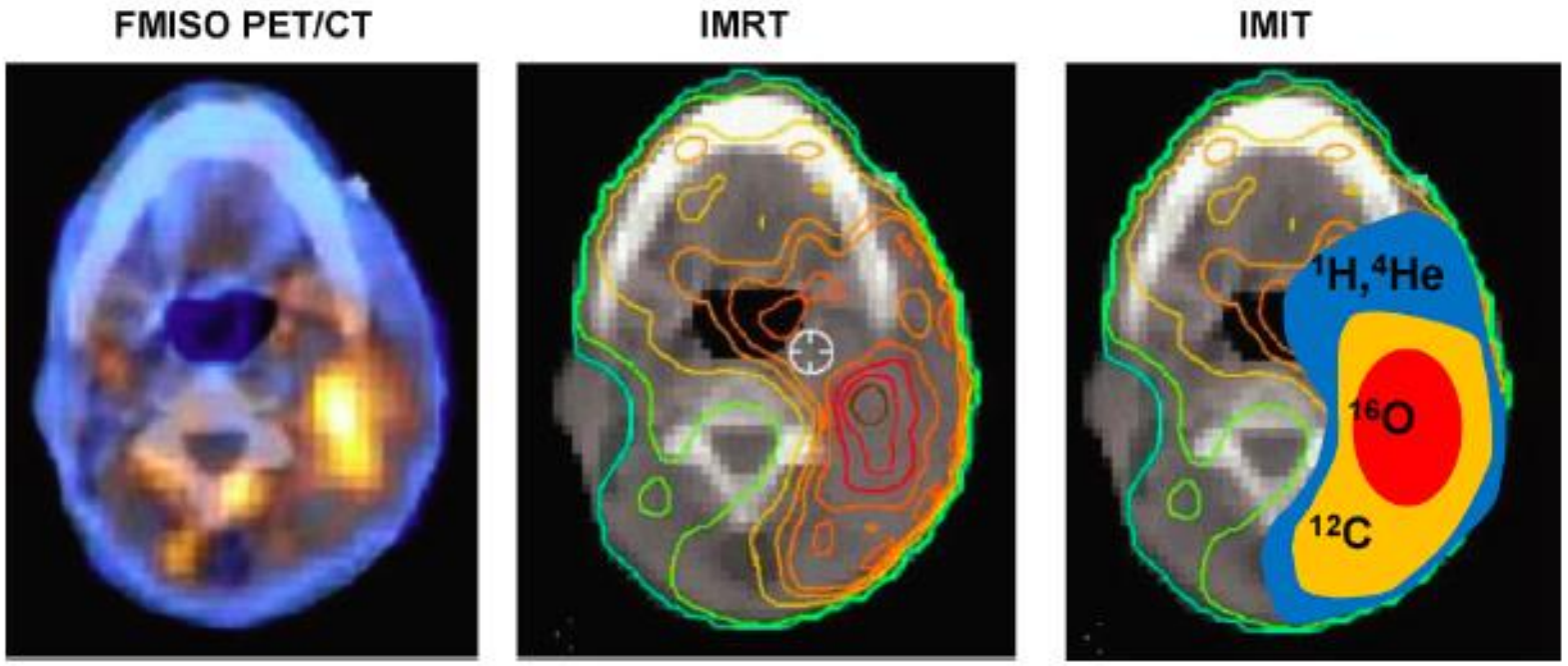

Example of hypoxia imaging based on FMISO PET/CT (left), and corresponding locally enhanced dose to hypoxic structures for dose painting in IMRT (middle), as well as illustrative implementation of radiation-quality-modulated dose painting in IMIT, targeting with heavier ions (16O, 12C) the most resistant (i.e., hypoxic) tumor subareas while keeping low-LET radiation in the surrounding tumor volume. Adapted with permission from D. Thorwarth and M. Alber, “Implementation of hypoxia imaging into treatment planning and delivery,” [Reprinted with permission from D.Thorwarth and M. Alber, Eberhard Karls University Tubingen (2011)].

[K.Parodi,Medical Physics, Vol. 42, No. 12, December 2015]

PRECLINICAL SYSTEMS
(from man to mice... and back)

IRIS PET System at Pisa

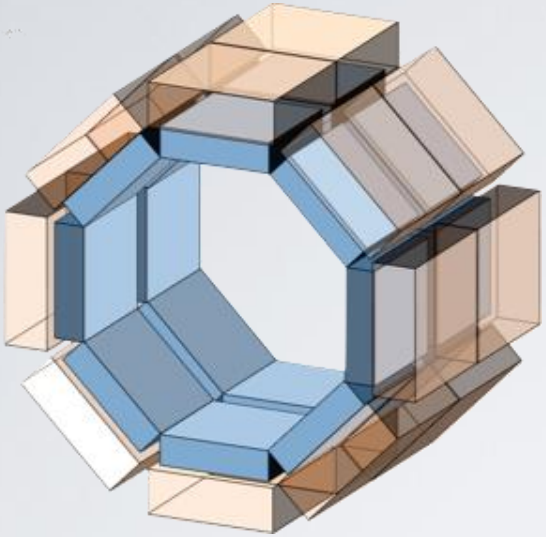

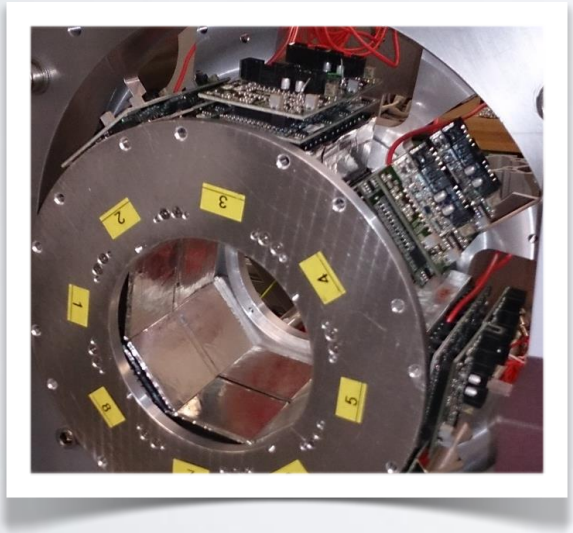

Detector module specifications	
Crystal material	LYSO:Ce
Crystal size (mm)	1.60 mm x 1.60 mm x 12 mm
Crystal pitch (mm)	1.68 mm
Crystals per module	27 x 26
Photodetector	MA-PMT 64 ch. (resistive chain readout)
System specifications	
No. of modules	16
No. of rings	2
Bore size (mm)	100 mm
FOV size (mm)	80 mm (T) x 95 mm (A)
Other features	
PET Detector rotation	

PET design and picture of the PET ring

PET/CT images with the IRIS PET/CT pre-clinical system at Pisa

Rotating acq.

Derenzo phantom image

- 2 MBq of ^{18}F
- 20 min. scan time

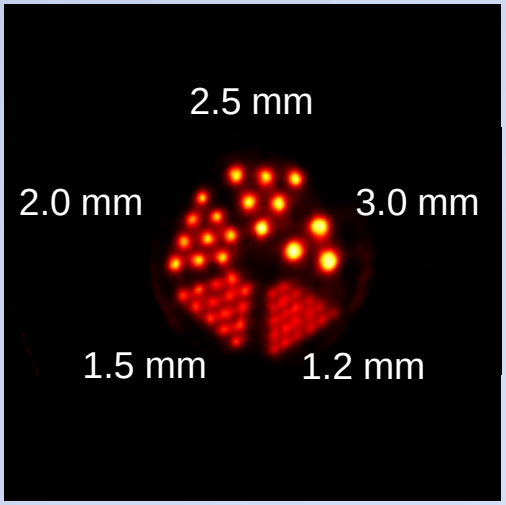

ML-EM reconstruction
70 iterations

All images displayed in a single slice with:
0.420 x 0.420 x 0.855 mm^3 voxel size

Static acquisition.

In-vivo Mouse image

- 2 MBq of ^{18}F-FDG
- 15 min. scan time

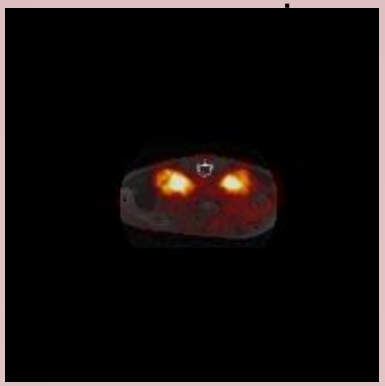

ML-EM reconstruction
70 iter. with 1mm (σ)
post smoothing

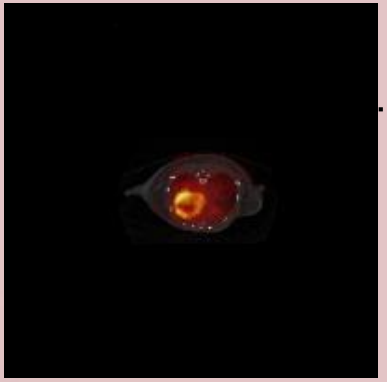

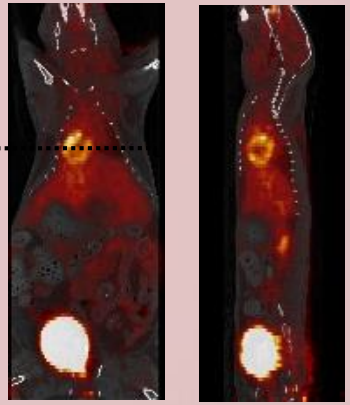

CT scan

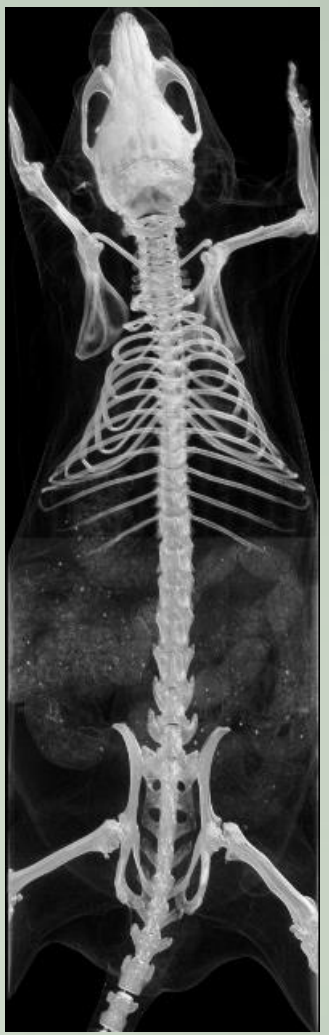

Single scan
FDK reconstruction
MIP projection

Cardiac (8 phases) and respiratory gating (binary) of a rat heart beating (18F-FDG)

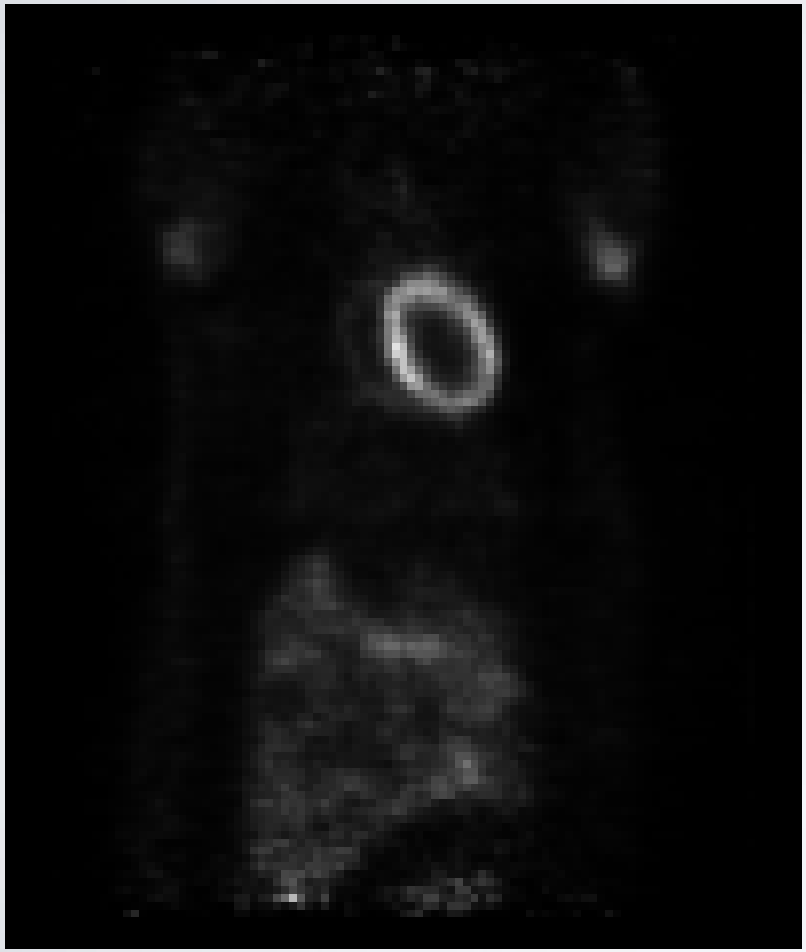

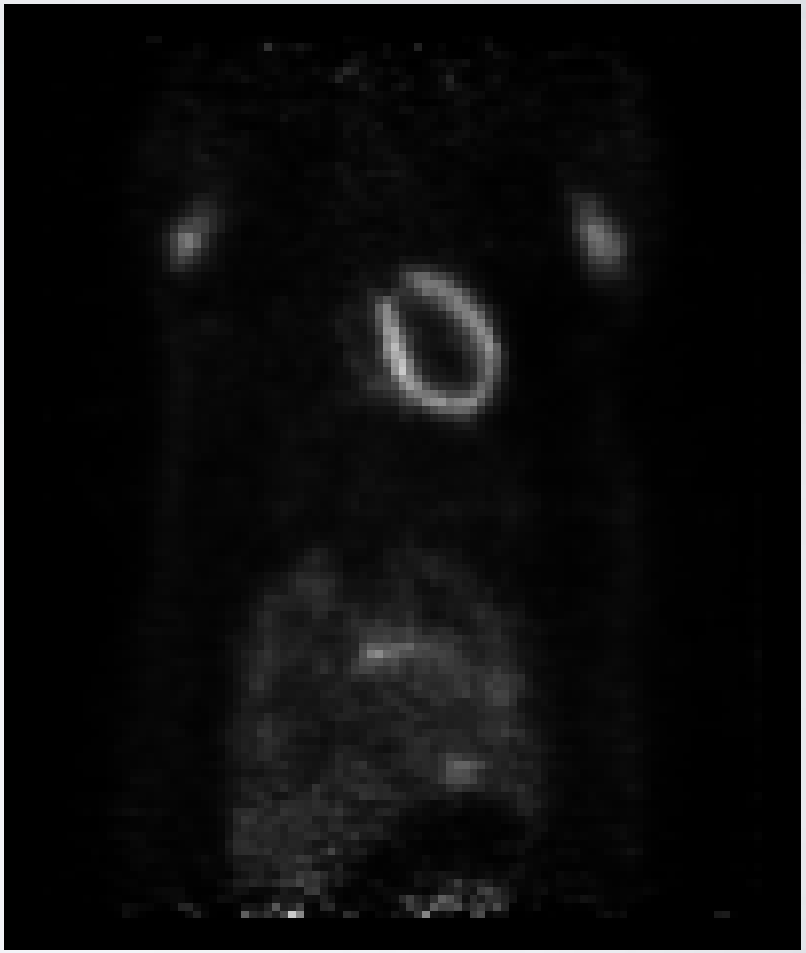

Taken with IRIS PET/CT scan:Courtesy of David Brasse, CNRS, Strasbourg (2016)

Organ specific PET

- **Breast (e.g. see talk onTu 3, @11.20 Auffray et al.)**
- **Prostate (e.g. see talk onTu 3, @11.40 Pizzichemi et al.)**
- **Brain (e.g. See TRIMAGE talk on Mo 2, @16.20 Del Guerra)**
- **Whole body PET ➔ Long axial PET**
  (e.g. see talk on We 4 @ 8.30 Moses)

..etc..

"Prior Art" upright brain PET imaging

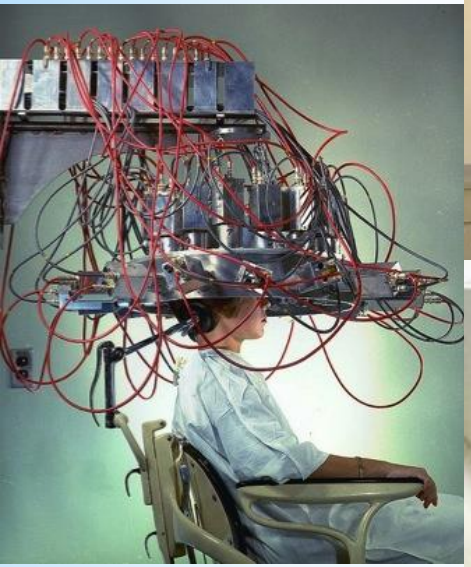

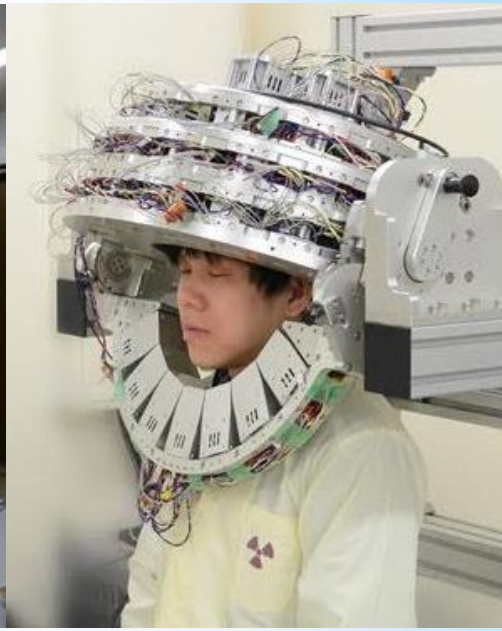

Left: 1961 – Brookhaven's "Headshrinker", Center-Left: 2011 – "PET-Hat". Center-Right: 2013 – Hamamatsu's brain PET system, Right: 2015, "Helmet-Chin". None compact, one wearable. (Courtesy of Stan Majewski, 2016)

Hybrid Systems
PET/MR

Why PET/MRI?

It all started with systems where PET and MRI are performed separately in time with distinct machines:

- Two images to be merged together
- Movements of the patient on the couch
- Data corruption from image fusion techniques

Philips Ingenuity TF PET/MR Combo

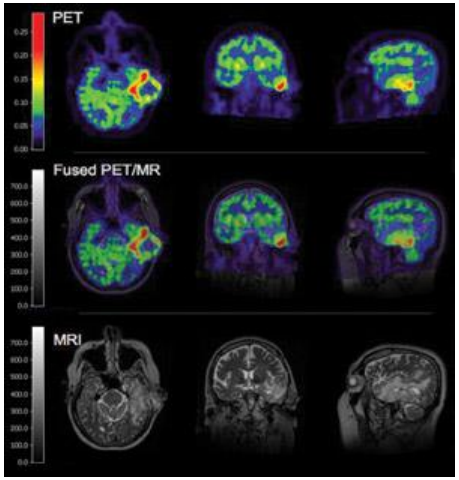

PET and MRI image fusion

PET-CT

PET-MR

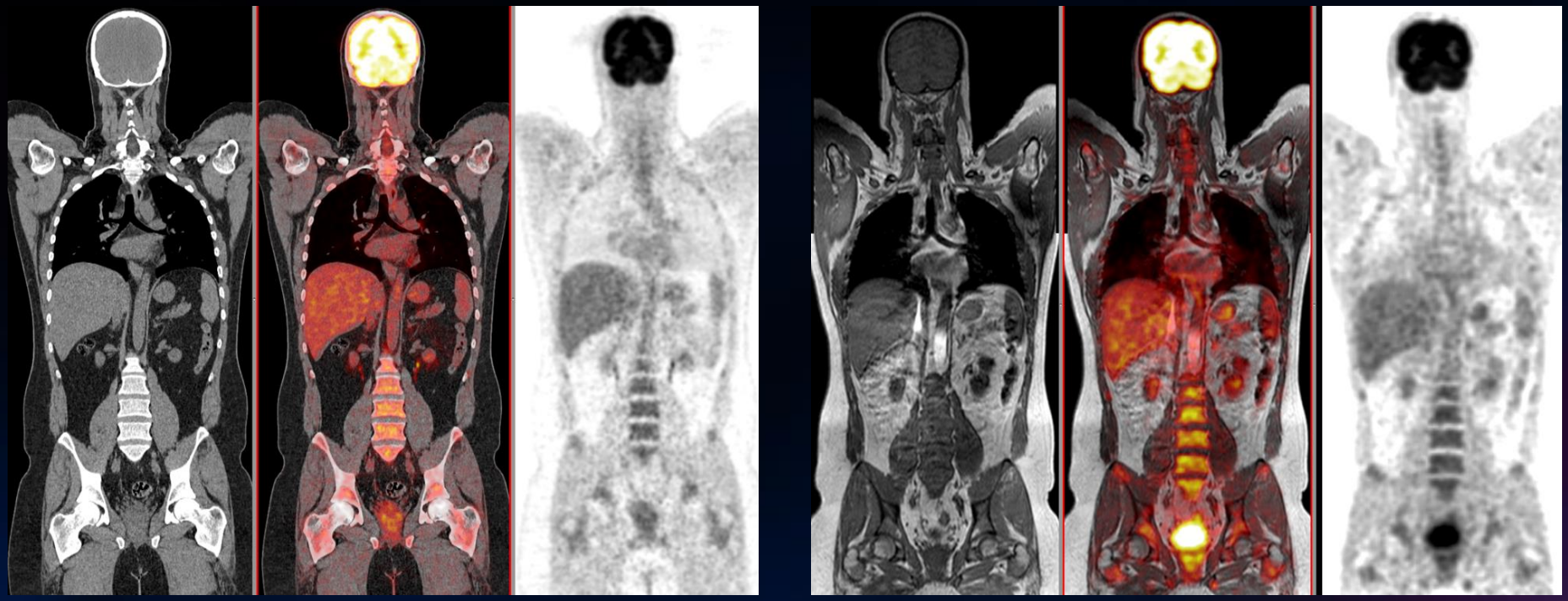

Representative clinical PET-CT (left) and PET-MR (right) whole-body images of the same patient acquired sequentially (~60 min time difference) on two combined systems (Siemens Biograph Hirez TrueV and Philips Ingenuity TF PET-MRI, respectively) following injection of 370 MBq of 18F-FDG.

[H.Zaidi and A.Del Guerra, Medical Physics, 2011, 38(10),5667-5689]

Why Combined PET/MRI?

Hybrid PET/MRI systems provide functional and morphological information *at the same time*:

- No image fusion required
- Space and costs saving
- Better soft tissue contrast
- Lower radiation doses

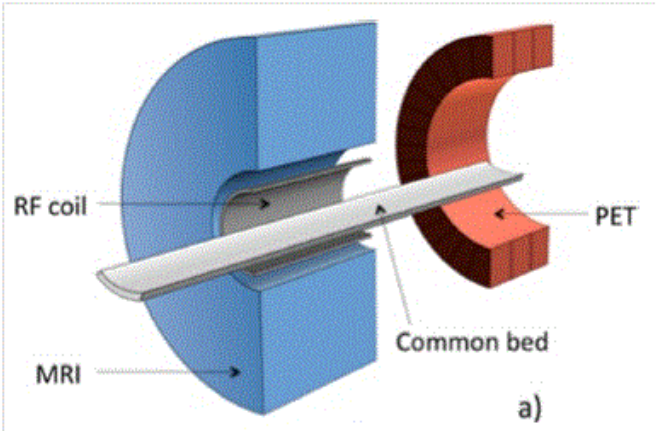

Tandem PET and MR configuration

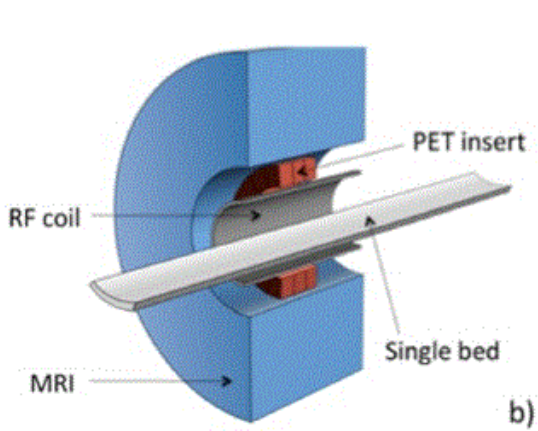

Hybrid PET/MR scanner

[H.Zaidi and A.Del Guerra, Medical Physics, 2011, 38(10),5667-5689]

PET inside a MR system

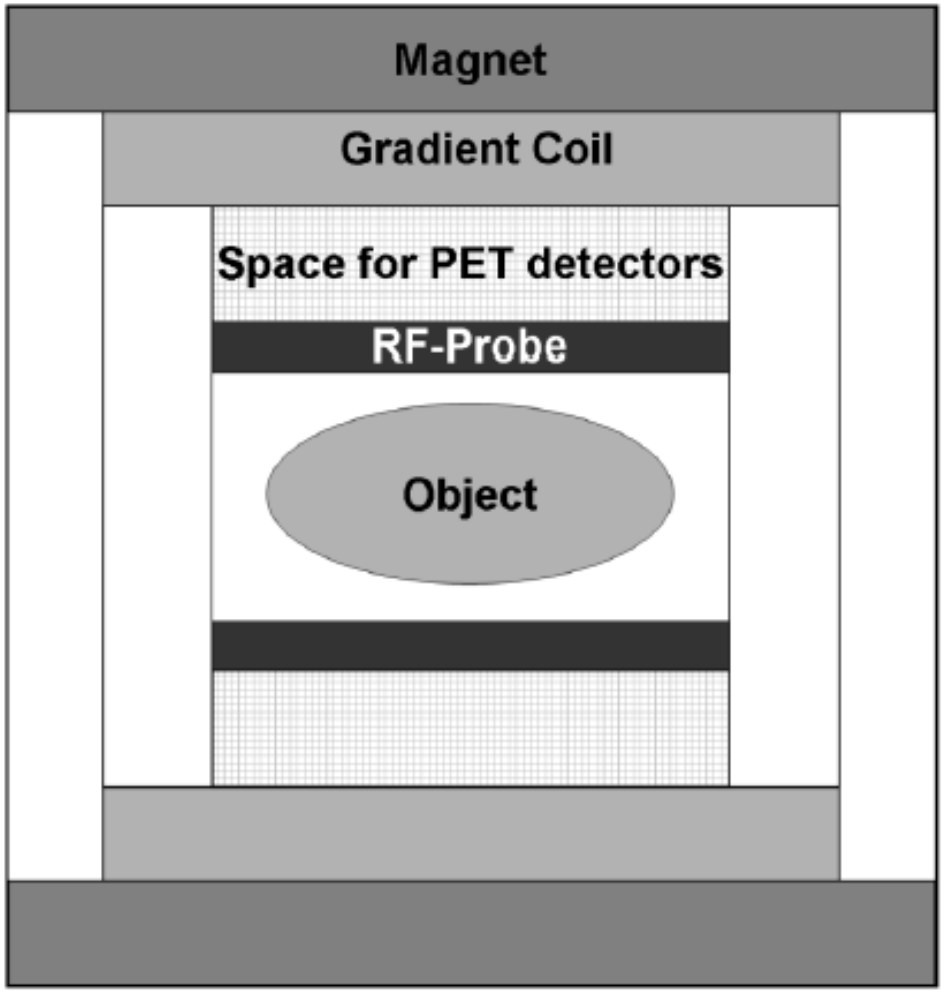

First APD based PET/MR scanner

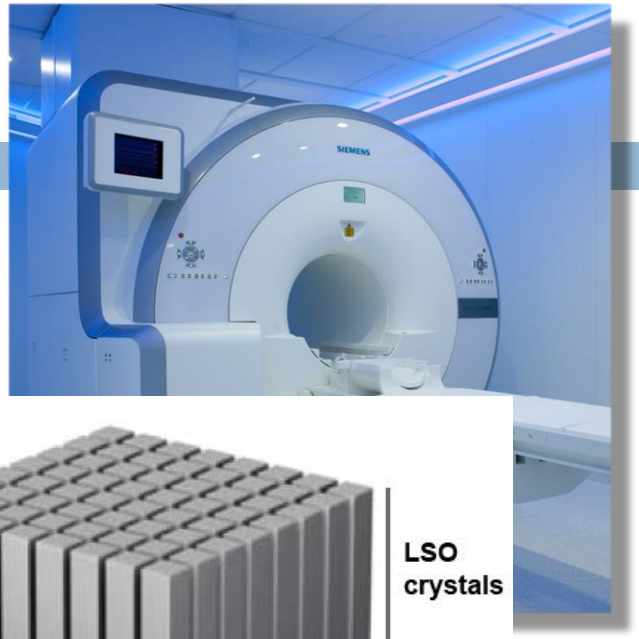

- Fully integrated whole-body PET/MR
- R[illegible]
  - PET:
    - 448 detector blocks wi
    - 8 x 8 LSO crystals and
    - 3 x 3 APDs each
    - Axial FOV: 25.8 cm
    - Spat. resolution: 4.3 mm

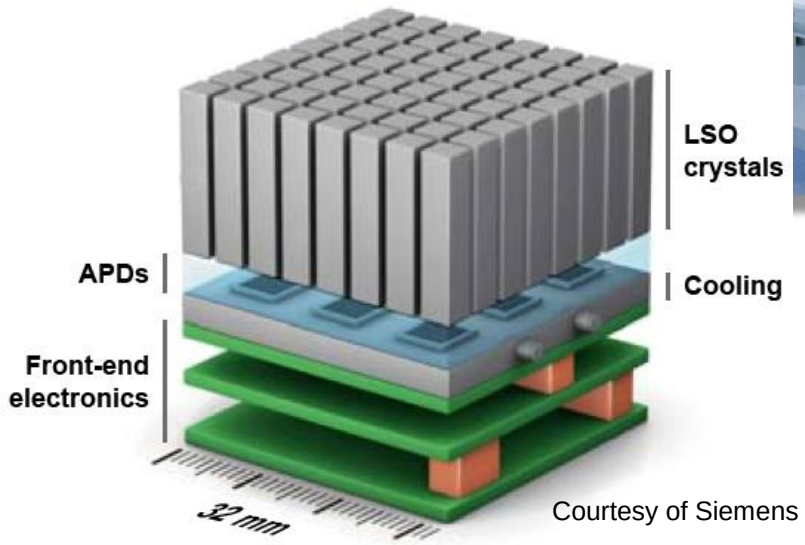

Courtesy of Siemens

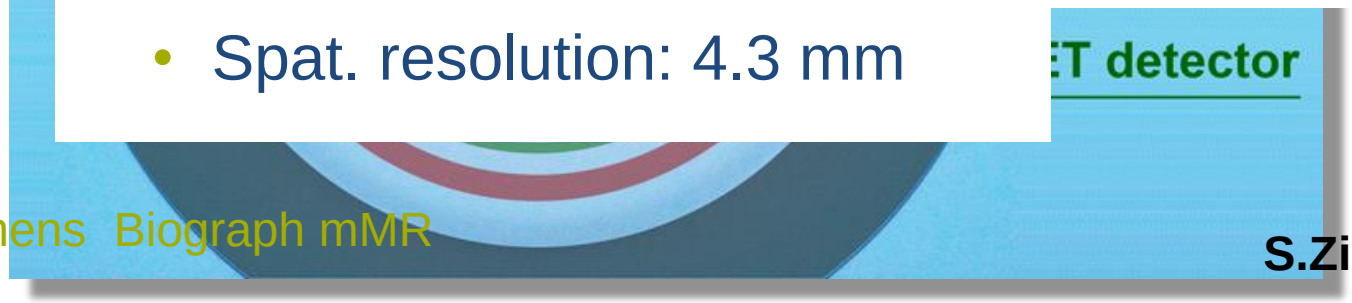

Siemens Biograph mMR

S.Ziegler, TUM, 2015

First SiPM based clinical scanner

GE Signa SiPM-based PET/MRI system

Based on Hamamatsu silicon photomultipliers (SiPMs)

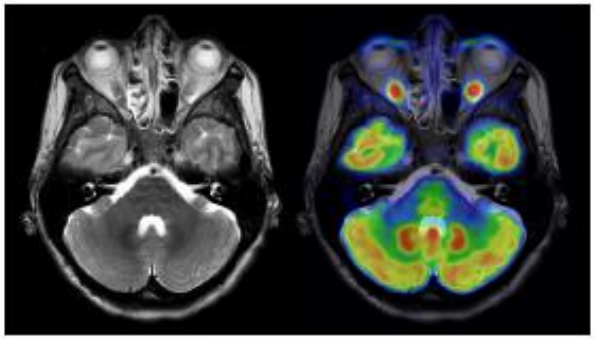

System Performance	
CRT	< 400 ps FWHM
Sensitivity	21 kcps/MBq
FOV	60 x 25 cm
Spatial res	4.1 mm
Energy res	< 12%

D. Schaart, Delft University of technology, 2015

TRIMAGE PROJECT

www.trimage.eu

Coordinator: Alberto Del Guerra (University of Pisa)

TRIMAGE: an optimized TRImodality (PET/MR/EEG) imaging tool for schizophrenia

- *TRIMAGE aims to create a trimodal, cost effective imaging tool consisting of **PET/MR/EEG** using cutting edge technology with performance beyond the state of the art.*

- *The tool is intended for broad distribution and will enable effective early diagnosys of schizophrenia and possibly other mental health disorders.*

WP3 Objective

Design and construction of a PET system capable to:

- Image the brain with a image quality beyond the state-of-the-art

- Operate inside a 1.5T MR

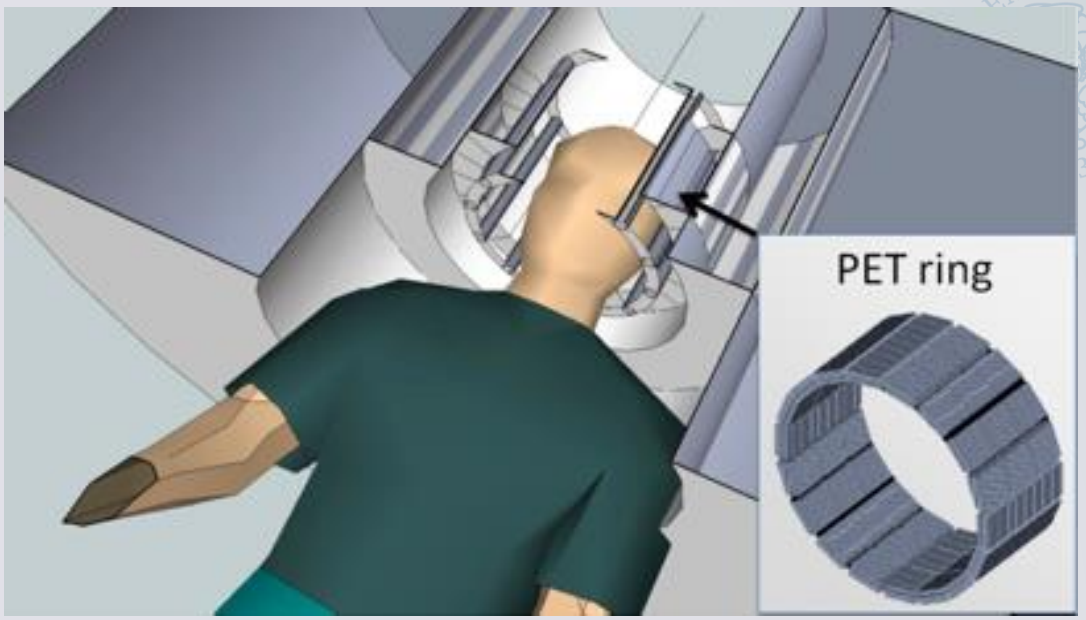

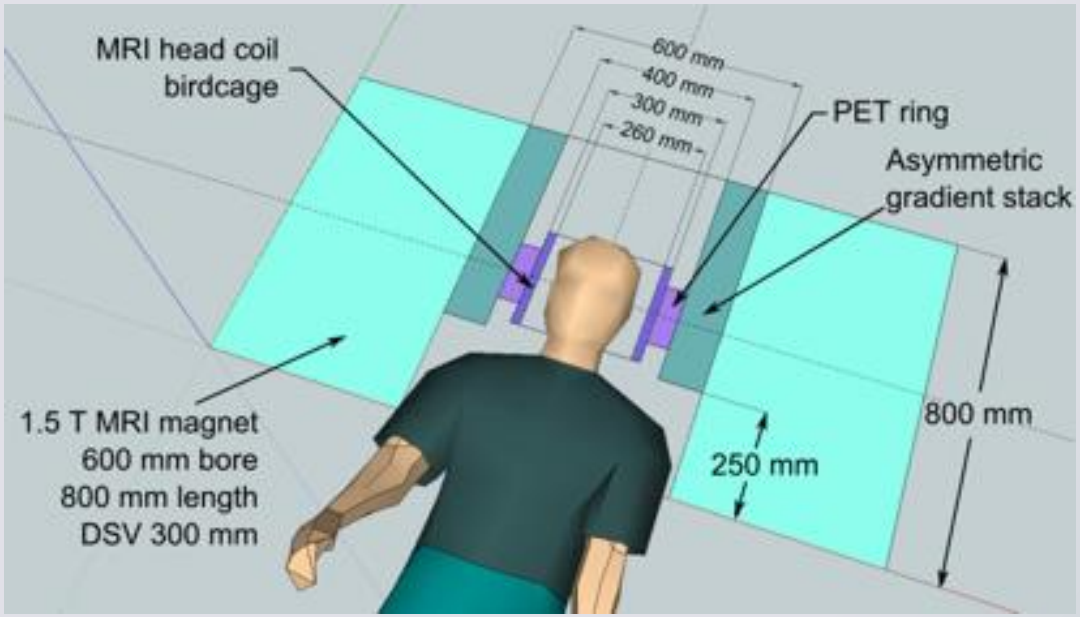

See talk on Monday 2 may @16.20-16.40

PET Range Monitoring in particle therapy

Tacking advantage of nuclear interactions

Activity of β^+ emitters

- Baseline approach
- Isotopes of short lifetime ^{11}C (20 min), ^{15}O (2 min), ^{10}C (20 s) with respect to diagnostic PET (hours)
- Low activity → long acquisition time (~minutes) with difficult in-beam feedback
- Metabolic wash-out of β^+ emitters

Prompt nuclear de-excitation γ's

- ~1-10 MeV
- emission profile correlated with dose profile
- Specific detector at present under development: collimated slit cameras or Compton cameras

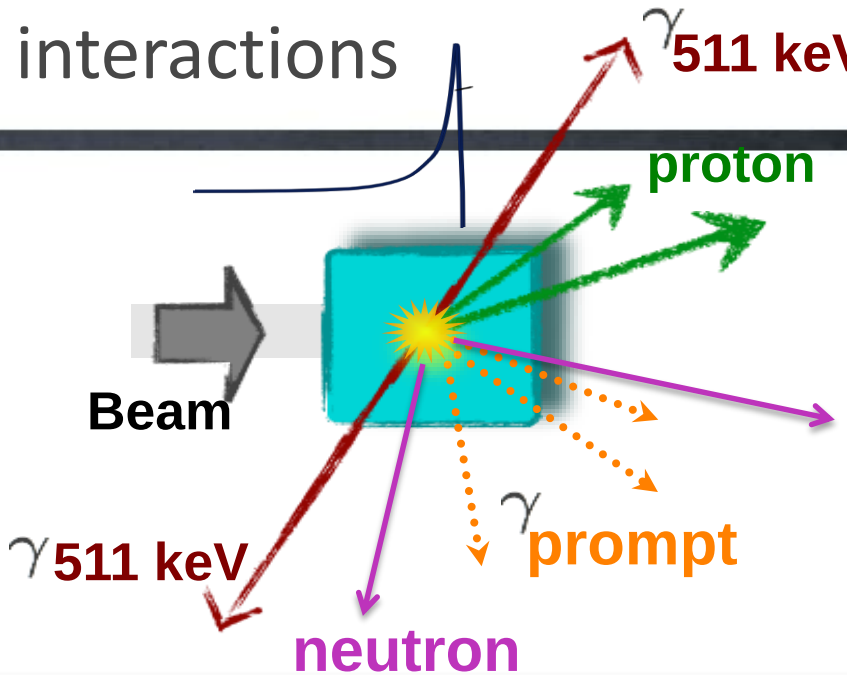

Charged secondary particles (ion therapy):

- The detection efficiency is almost one
- Can be easily back-tracked to the emission point -> can be correlated to the beam profile & BP
- They are forward peaked
- Enough energy to escape from patient
- MS inside the patient -> worsen the back-pointing resolution

Positron Emitters and PET imaging

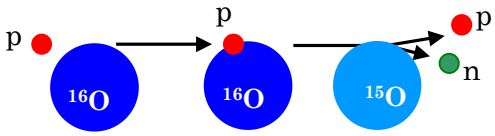

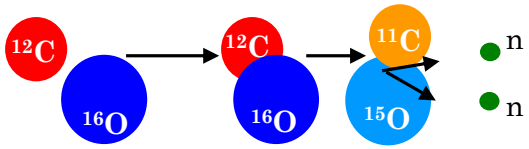

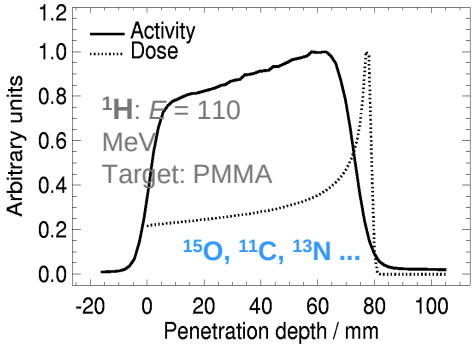

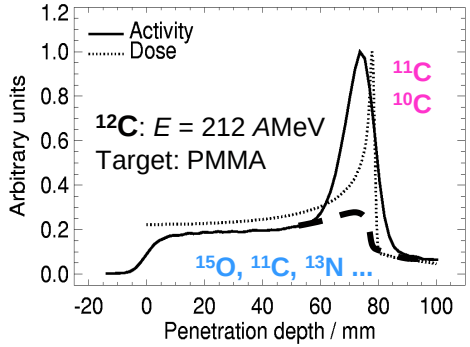

- **A possible method for the control of the geometrical accuracy of the treatment (TPS) is PET imaging of the activity generated in the nuclear interactions in tissue**

- **Small amounts of β^+ emitting radioisotopes are produced with short half-lives**
  - **^{11}C (20.3 min)**
  - **^{13}N (9.97 min)**
  - **^{15}0 (2.03 min)**

38

State of art of PET monitoring

Xuping Zhu and Georges El Fakhri, Proton Therapy Verification with PET Imaging, Theranostics. 2013; 3(10): 731–740.

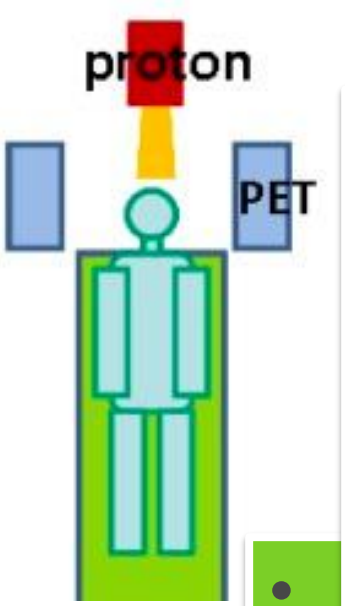

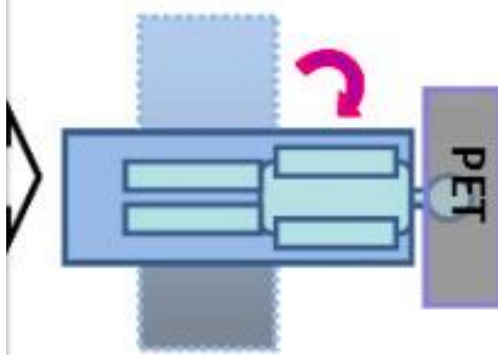

- In-beam PET
  - First pioneer work by Enghardt et al. In the '90 with C ions (GSI/Bastei Tomograph)
  - HIMA, Chiba, Japan
  - NCC, Kashiwa, Japan w proton beams
  - "OpenPET", NIRS, Japan
  - DoPET at the CATANA Protontherapy Center in Catania, Italy
  - INSIDE at CNAO in Pavia, Italy

- m PET
  - ET (now full PET
  - egrating CT) at
  - SA

DoPET(University of PISA & INFN)

DoPET is a stationary 2 heads tomograph

- **gantry compatibility**
- **in-beam acquisition**

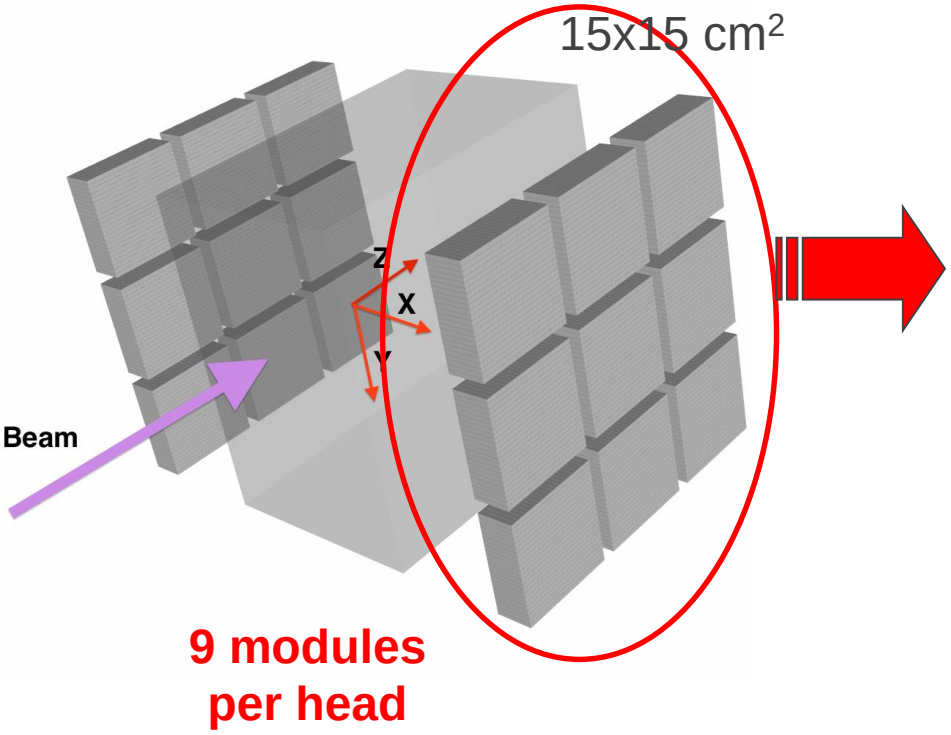

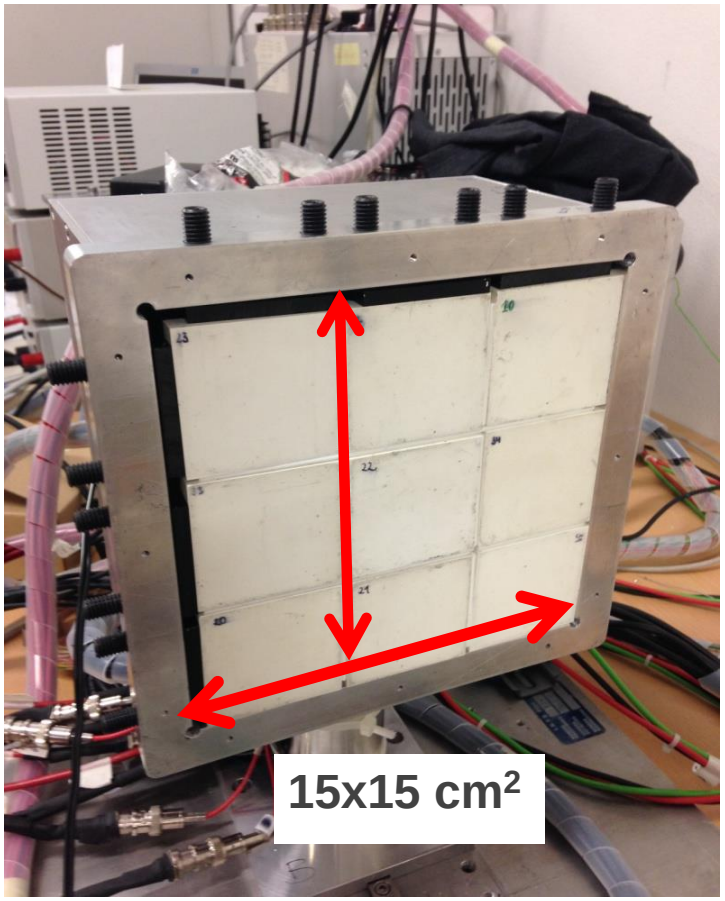

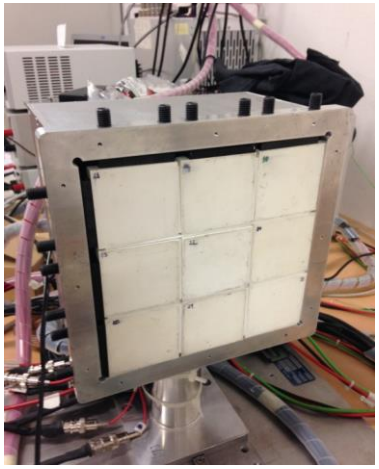

DoPET (9 vs 9 modules) [15cmx15cm vs 15cmx15cm]

The current prototype is an upgrade of a previous 4x4 system

S,Vecchio, IEEE Trans. Nucl. Science, 56 (1), (2009)
G.Sportelli, IEEE Trans. Nucl. Science 58 (3) (2011)

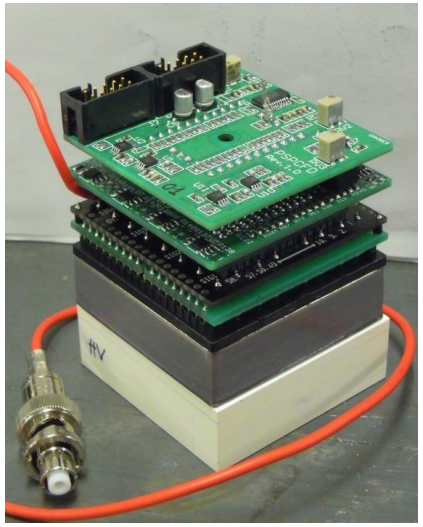

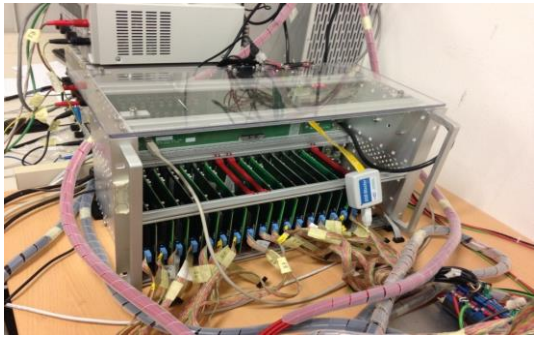

- **Hardware (9x9 modules)**
  - *Each detecting module made of*
    - *one LYSO matrix (23 x 23 crystals, 2mm pitch)*
    - *one PS-PMT 8500 Hamamatsu*
    - *Dedicated front-end electronics*
  - *FPGA based acquisition and coincidence processing (Coincidence time window ~5 ns).*

- **Software:** Activity reconstruction algorithm:
  - Maximum Likelihood Estimation Maximization (MLEM)
  - The reconstruction is performed in few minutes➔ We are working on implementing GPU for bringing the reconstruction time down to 30s

PET Imaging with various energy ion beams (12-C and p @CNAO)

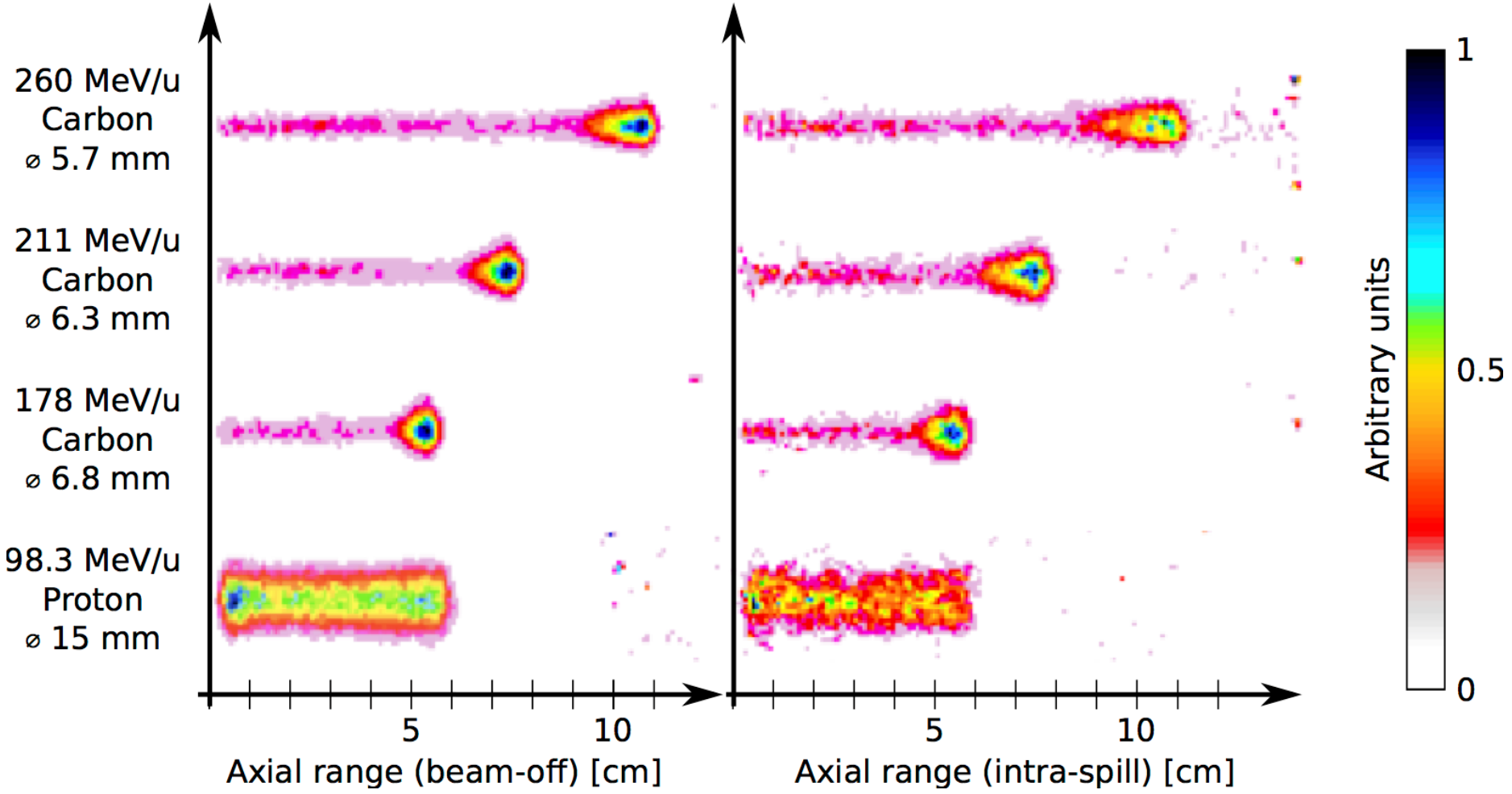

[G.Sportelli et al., JINST, 2016 (in press)]

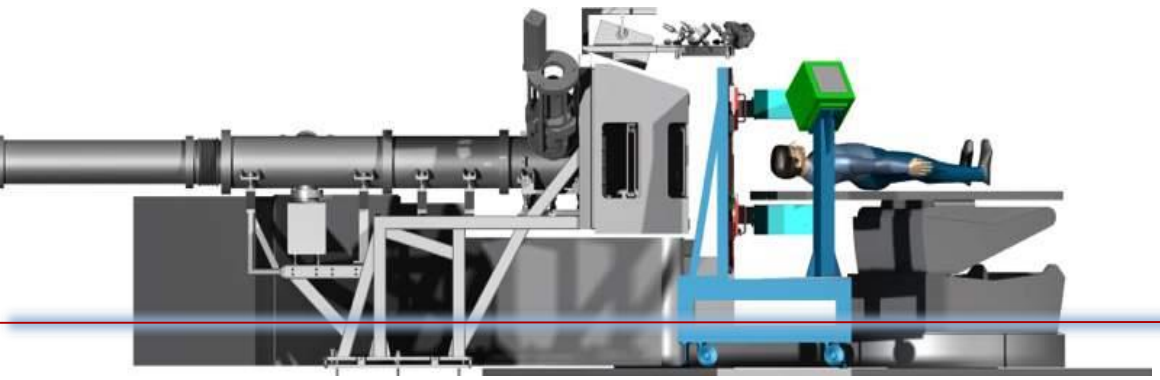

INnovative Solutions for In-beam DosimEtry in Hadrontherapy

Pisa,Torino,Roma"La Sapienza",Bari,INFN

INSIDE coordinator: M. G. Bisogni (Pisa)

This project has been supported by Italian MIUR under the program PRIN 2010-2011 project nr. 2010P98A75 and by EU FP7 for research, technological development and demonstration under grant agreement no 317446 (INFIERI)

N. Belcari, N. Camarlinghi, A. Del Guerra, S. Ferretti, E. Kostara, A. Kraan, B. Liu, N. Marino, M. Morrocchi, M.A. Piliero, G. Pirrone, V. Rosso, G. Sportelli

P. Cerello, S. Coli, E. Fiorina, G. Giraudo, F. Pennazio, C. Peroni, A. Rivetti, R. Wheadon, A. Attili, S. Giordanengo

E. De Lucia, R. Faccini, P.M. Frallicciardi, M. Marafini, C. Morone, V. Patera, L. Piersanti, A. Sarti, A. Sciubba, C. Voena

F. Ciciriello, F. Corsi, F. Licciulli, C. Marzocca, G. Matarrese

G. Battistoni, M. Cecchetti, F. Cappucci, S. Muraro, P. Sala

partners: CNAO

In-beam PET heads

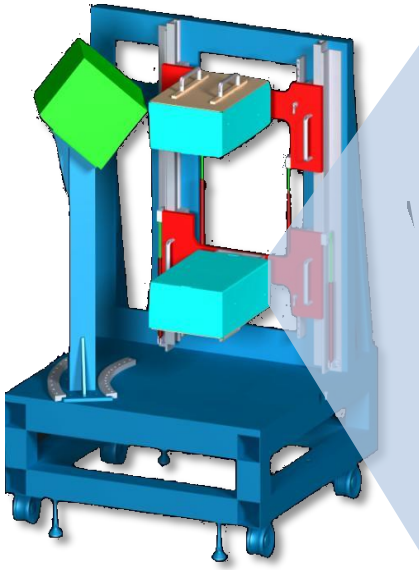

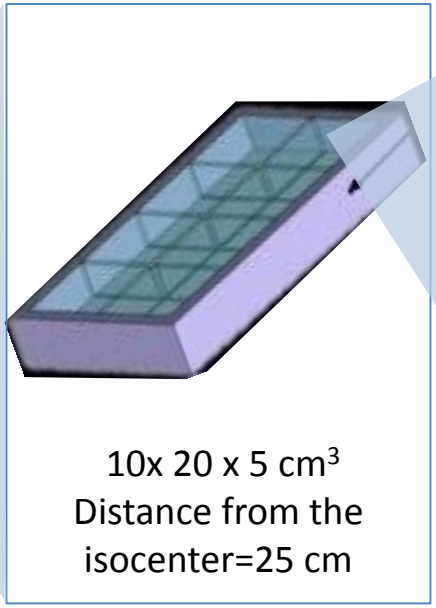

10x 20 x 5 cm^3
Distance from the isocenter=25 cm

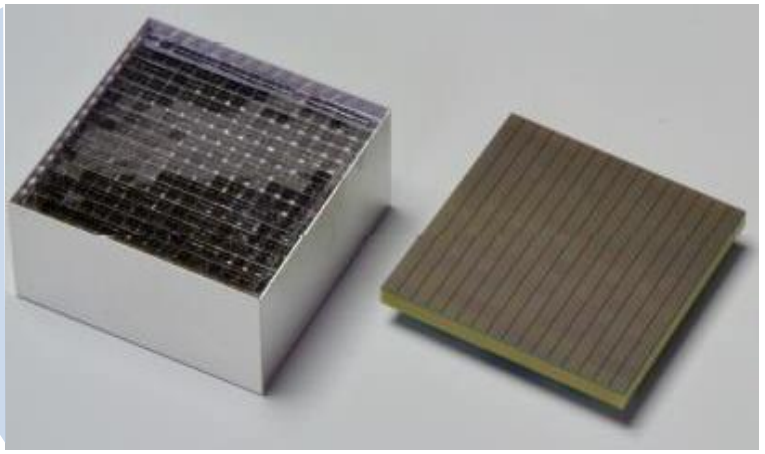

256 LFS pixel crystals (3x3x20mm^3) coupled one to one to MPPCs (Multi Pixel Photon Counters, SiPMs).

Solid model Of the PET head

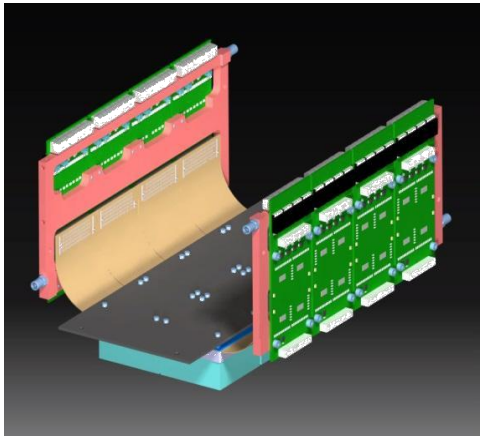

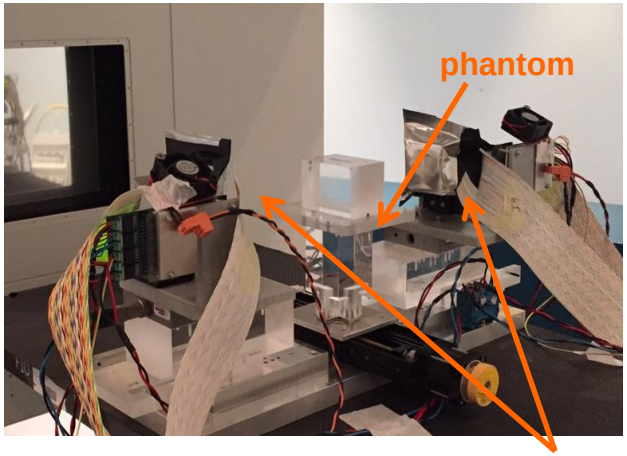

Demonstrator
1 vs 1 module
Tested at CNAO
On May 5 2015

Work partly supportedd by the European Union EndoTOFPET-US project and by a Marie Curie Early Initial Training Network Fellowship of the European Union 7th Framework Program (PITNGA-2011-289355-PicoSEC-MCNet).

Activity profile / interspill data

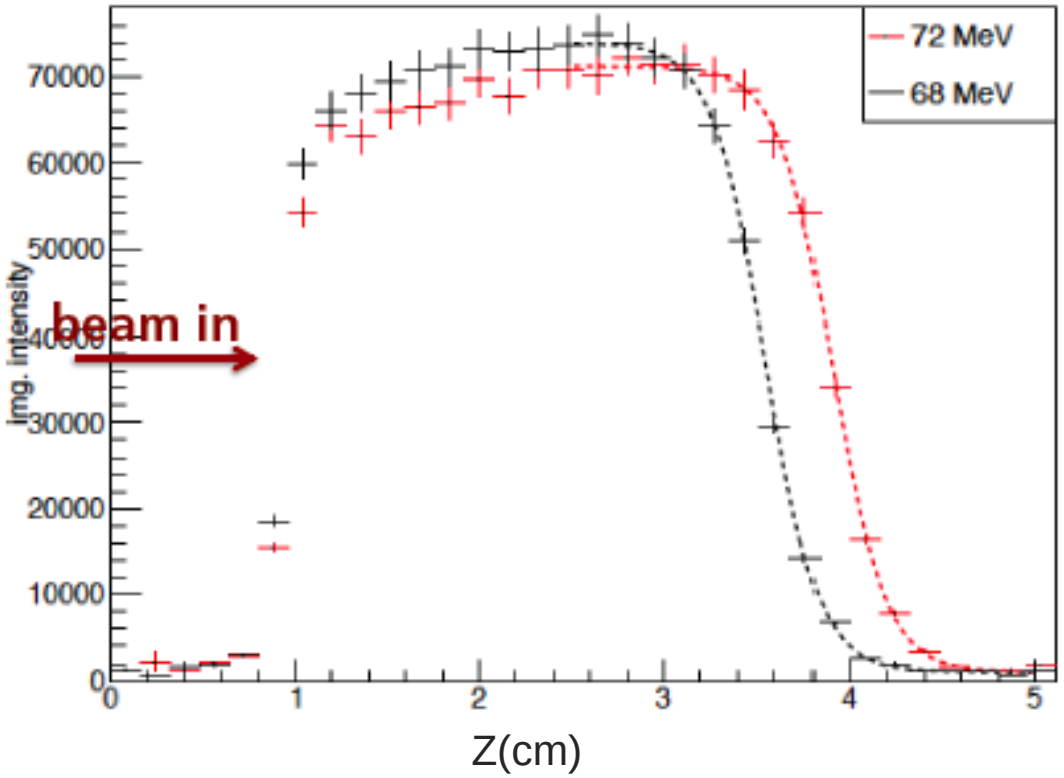

PMMA phantom
Difference in the distal fall-off

Expected:
3.7 mm
Measured:
(3.6 +/- 0.3) mm

Francesco Pennazio, INFN and Uni Torino, Italy

The full PET system installed at CNAO 7/2/2016

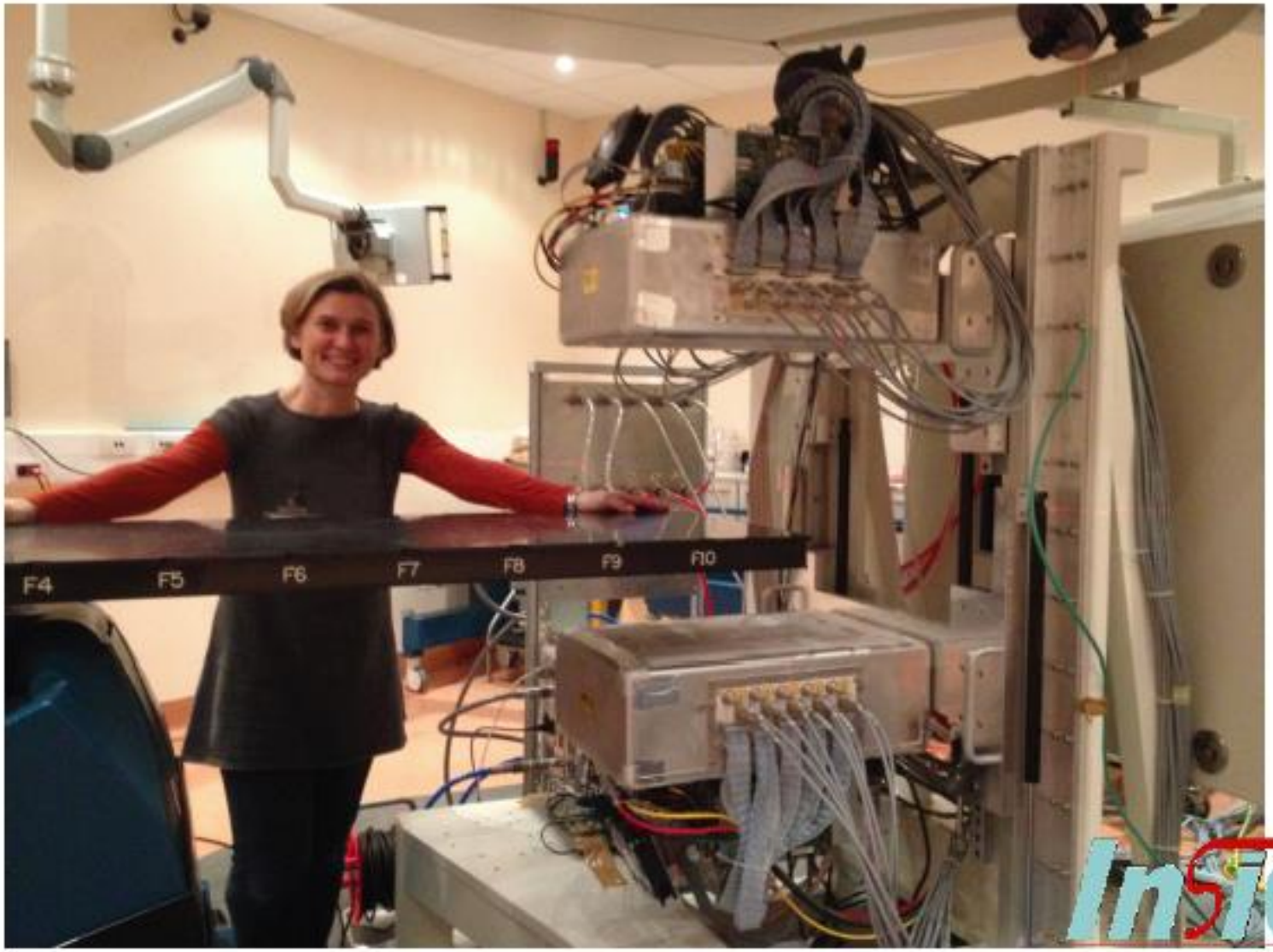

First image taken on a Rando Phantom @CNAO (April 2016)

TPS with proton for a nose-pharinge tumor
PET Detector full size: 10 cm x 20 cm

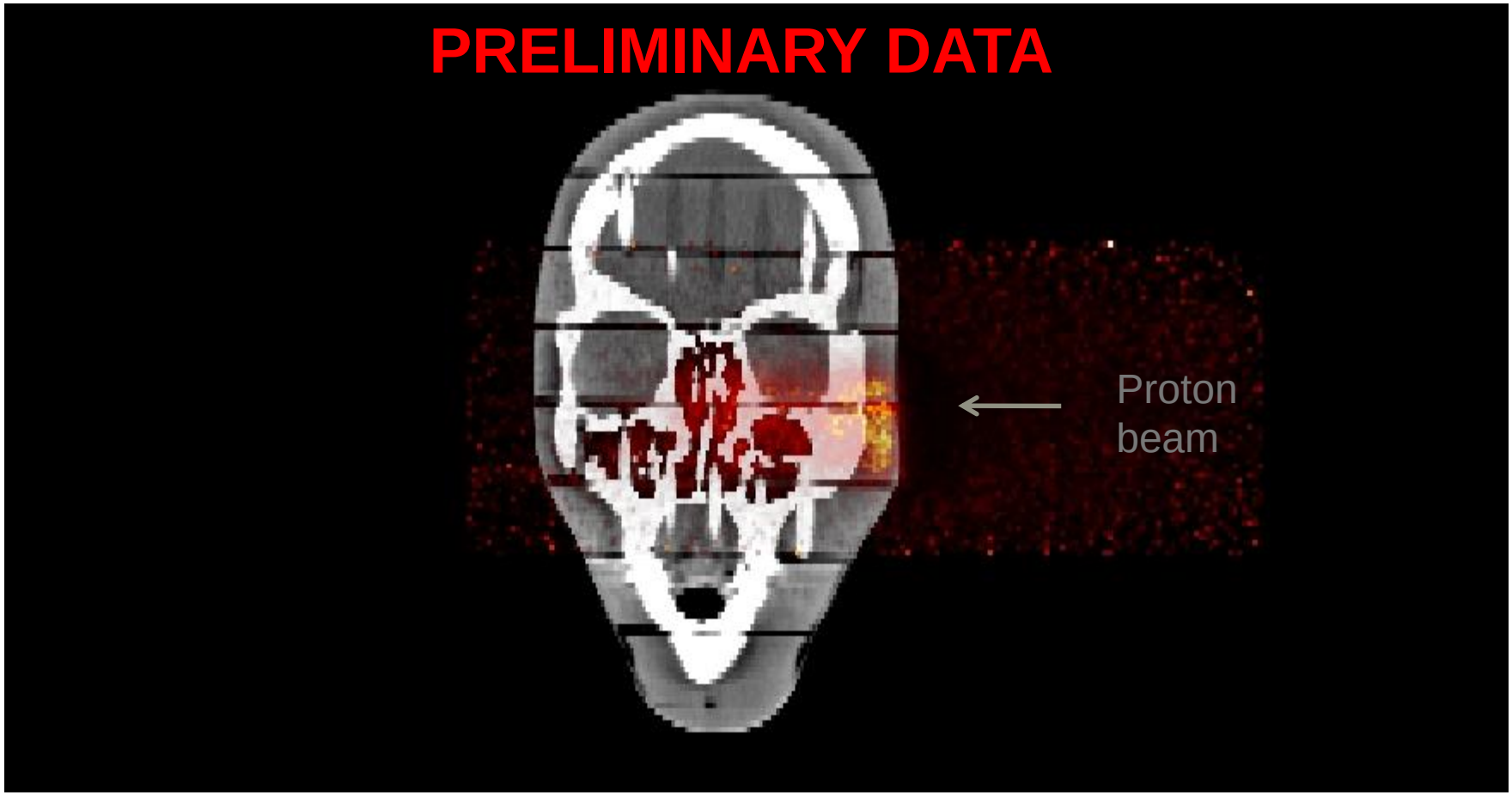

CONCLUSIONS

Take home message #1

• Technological aims	PET detector performance	ITEMS addressed
•Increase Sensitivity	➔ Reduce dose ➔ Increase Image quality ➔ Increase throughput	Long Axial whole body PET for oncology
• Increase spatial resolution	➔ Improve quantitation (i.e.,recovery coefficients)	Monolithic crystal + Digital SiPM in CMOS
• Increase time resolution (TOFPET)	➔ Increase S/N ➔ sensitivity ➔ Direct 3D imaging	Digital SiPM in CMOS + FPGA electronics [Cerenkov PET(?)]
• Improve algorithms	➔ Improve clinical response	OSEM with full PSF Parametric reconstruction
• Improve radiotracer	➔ Simultaneous multifunctional studies	Multimodal xPET/MR
Last, but not least	➔ Understand the clinical problem!!	Sinergy!!

Understanding the clinical problem

TRANSLATING TECHNOLOGY FROM NUCLEAR AND PARTICLE PHYSICS TO THE CLINIC: ADDRESSING MEDICAL NEEDS BY DETECTOR KNOW-HOW WITH A FOCUS ON ORGAN-SPECIFIC IMAGING

Hey, I've solved your clinical problem

Physicist

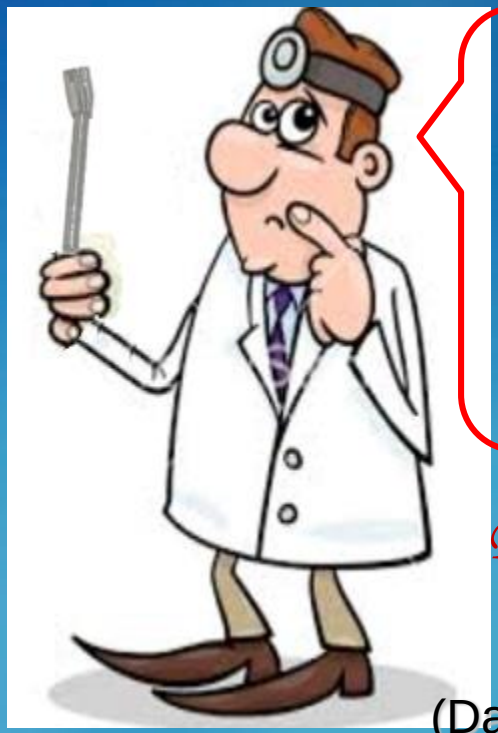

I didn't know I had a problem

Physician

(David Townsend)

UNIVERSITY of VIRGINIA HEALTH SYSTEM

Take home message #2

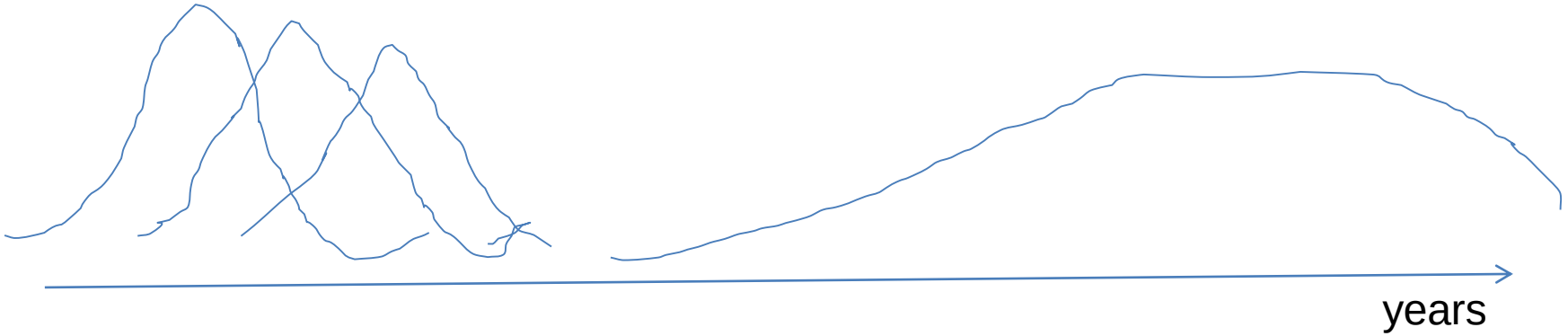

Consumer cycle: 3 y **Medical device cycle 15-20 y**

- Technology Transfer in the medical field needs long term investment
- Industry can withdraw half-way through, if not profitable,e.g. Siemens for proton therapy

Ref: From the keynote talk by Dr. Jaemoon Jo (SamsungSenior Vice-President) at MIC_2013, Seoul

CONCLUSIONS

- **After 65 years PET is alive and kicking and it is fundamental for precision medicine.**
  ➔ It's no time for retirement!

- **Organ specific PET devices (whole body, breast, brain, prostate, pediatric PET, range in hadrontherapy..)**

- **Multimodality Imaging (PET-CT, PET-MR, PET-US,..and more)**

THANK YOU
for your attention!

Questions?